ACS Sustainable Chemistry & Engineering

Research Article

pubs.acs.org/journal/ascecg

Template Free Synthesis of Ni-Perovskite: An Efficient Catalyst for Hydrogen Production by Steam Reforming of Bioglycerol

S. Ramesh[†] and N. J. Venkatesha*[,‡]

[†]IMCN/MOST, University of Catholiquic de louvain, Louvain-la-nueve, Belgium 1348

[‡]Chemistry Research Center, Bangalore Institute of Technology, K.R. Road, V.V Pura, Bengaluru-560004, India

ABSTRACT: Ni-based perovskite catalysts are prepared by two different methods and used as selective catalyst for hydrogen production from glycerol. The physicochemical properties of the catalysts were studied by X-ray diffraction, H_2 temperature-programmed reduction, NH_3 temperature-programmed desorption, N_2 physisorption and TEM analysis. The effects of perovskite structure on the Ni particle size and acidity were studied, and the possibility of a nontemplate approach is examined. Steam reforming of bio-glycerol was carried out in a fixed bed down flow reactor at atmospheric pressure. The catalysts were compared with the Ni supported alumina; catalysts prepared with and without template were found to contain smaller nickel oxide particles and optimum acidity for good glycerol conversion and hydrogen selectivity. Under optimized reaction conditions, $LaNiO_3$ (E) catalyst exhibited 72% glycerol conversion with 70% hydrogen selectivity. The Ni/Al_2O_3 catalyst with bigger nickel oxide particle size and moderately strong acidic sites results in quick deactivation, metal sintering, and predominantly filamentous carbon deposition due to the coke formation.

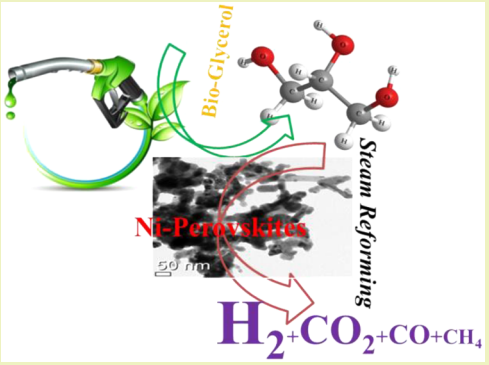

KEYWORDS: *EDTA, Ni particle size, Deactivation, Hydrogen selectivity, Acidity, $LaNiO_3$*

1. INTRODUCTION

Hydrogen is recognized as one of the promising fuels of the future due to its high energy density, cleanness and recyclability.[1,2] Because of the intrinsic drawbacks of fossil fuels having limited sources as an environmental concern, the demand for renewable energy sources is rapidly growing technology for upcoming decades.[2] Nowadays hydrogen is mainly produced by the reforming of natural gases, but this process does not contribute to the reduction of the greenhouse effect on sustainable development of the global economy.[3−5] The production of hydrogen from renewable sources, especially from biomass, attracted researchers from the past decade.[6−8] Among the biomasses, glycerol is a promising one, due to its nontoxic and relatively high hydrogen content and because it is produced as a byproduct during the biodiesel synthesis. Glycerol can be utilized to convert various valuable chemicals, and among those hydrogen has more precedence than others.[9,10]

Steam reforming of glycerol is a clean technology to produce hydrogen, and this reaction is conducted under ambient pressure and high temperature operation due to its endothermic nature.[11,12] Many transition metals are active toward steam reforming reactions. Among those, nickel based catalysts attained more interest due to their lower cost and effectiveness in breaking the C−C, C−H, and C−O bonds.[13−17] Conventionally, group VII metal ions supported on various supports such as alumina, silica, magnesia, ceria, and zirconia are reported as active catalysts for reforming, syngas conversion, dehydrogenation, and dehydration reactions.[18−23] Among them, the alumina supported one attained the greatest interest due to its larger surface area and porous nature.[22−24] Hence, development of stable, coke resistant, and cheap catalyst for steam reforming of glycerol remains a challenge for many researchers. However, the main drawback of nickel supported alumina catalyst leads to rapid catalyst deactivation because of the carbon deposition and sintering of the active Ni component at high temperature.[19−25]

Many researchers have studied the addition of other metal ions Sr,[26] Ca,[27] and Mg[28,29] to increase the stability of nickel supported alumina catalysts. In this regard, recently many catalysts have been reported as efficient catalysts for the steam reforming.[30] Perovskite type oxide catalysts have received much attention for steam reforming reactions due to their special properties.[31−33] These mixed metal oxides with well-defined cubic structure are capable of producing well-dispersed metallic particles during the reduction and avoiding carbon formation, leading to superior catalytic activity and stability at lower temperature.[34−38] The $LaNiO_3$ perovskite catalyst structure was widely studied, after reporting nickel supported alumina for hydrogen production by steam reforming of biowaste materials.[39] Recently Wu et. al[14] reported perovskite derived catalyst for steam reforming of glycerol at lower temperature,

Received: July 25, 2016
Revised: October 13, 2016
Published: December 27, 2016

 © 2016 American Chemical Society

DOI: 10.1021/acssuschemeng.6b01744
ACS Sustainable Chem. Eng. 2017, 5, 1339−1346

and they found that the stability can be improved by incorporation of other metal ions into the perovskite structure. Also, nickel particle size played a major role in the reforming reactions to achieve good activity and stability.[14]

In order to improve the stability of the perovskite derived nickel catalysts in steam reforming of glycerol, we prepared perovskite catalysts by two different methods, with and without templates, to generate catalysts with different nickel oxide particle sizes. The prepared catalysts were characterized, and their catalytic activities were studied in glycerol steam reforming at moderately lower temperature. Also, Ni supported alumina catalyst was prepared by the impregnation method and used for comparison.

2. EXPERIMENTAL SECTION

2.1. Preparation of the Catalysts. $LaNiO_3$ perovskite was prepared without using template through coprecipitation method.[12] Initially aqueous solutions of lanthanum nitrate hexahydrate and nickel nitrate hexahydrate were mixed in a 1:1 molar ratio. An aqueous solution of NaOH (3.2 M) was added dropwise for 1 h to get the precipitate, and it was filtered and repeatedly washed with deionized water. The residual part was dried overnight at 110 °C. Finally, the sample was calcined at 400 °C for 2 h and then at 700 °C for 6 h with a heating rate of 5 °C min^{-1}. The resulting catalyst was designated as $LaNiO_3$.

Similarly, an aqueous solution of lanthanum nitrate hexahydrate and nickel nitrate hexahydrate were mixed in a 1:1 molar ratio, and cellulose was added by stirring and ethylenediaminetetraacetic acid (EDTA)−ammonia solution was added dropwise to adjust the pH of the mixture to 5. The resulting mixture was aged for 3 h and dried at 110 °C overnight. Further calcination was made in the same way as for $LaNiO_3$, and the resulting catalyst was designated as $LaNiO_3$ (E).[14]

The reference catalyst Ni/Al_2O_3 was prepared by the wet impregnation method. A typical procedure involved the required amount of nickel nitrate hexahydrate to be dissolved in water. Then the preactivated alumina (540 °C for 4 h) was added, stirred for 3 h, after that dried at 110 °C overnight, and calcined at 700 °C for 6 h; the sample was designated as Ni/Al_2O_3.

2.2. Catalyst Characterization. XRD measurements were performed for fresh and spent catalysts, with 2θ values between 10−80° using a Rigaku C/max-2500 diffractometer having graphite filtered Cu Kα radiation (λ = 1.5406 Å). The Debye Scherer equation was used to estimate the mean NiO crystallite size based on the diffraction peaks of the Ni(200) plane.

The temperature-programmed reduction (TPR) experiments were carried out using a temperature program analyzer (BELCAT, BEL Japan, Inc.). Typically, 0.1 g of calcined sample was placed between quartz wool in a U-shaped quartz tube. The sample was thermally treated under an Ar stream at 400 °C for 2 h to remove physisorbed water and other gaseous impurities. The catalysts were cooled to room temperature under Ar gas. The pretreated sample was heated to 900 °C with heating rate 10 °C min^{-1} under a 5% H_2/Ar flow of 30 mL min^{-1}.

Textual properties of the catalysts were studied using a Quanta Chrome NOVA 1000 surface analyzer by nitrogen adsorption at −196 °C. Prior to measurement, samples were degassed to remove preadsorbed gas and moisture at 300 °C for 4 h. This instrument employed the BET method by measuring the quantity of nitrogen absorbed, and the cumulative volume and diameter of pores were obtained by the BJH method from the desorption isotherms.

NH_3 temperature-programmed desorption (TPD) was conducted by a Micromeritics Auto Chem II instrument. The powdered sample (300 mg) was first prereduced with 10% H_2/Ar at 700 °C for 1 h and then flushed with Ar at 700 °C for 30 min. Upon cooling to 100 °C, the sample was saturated with NH_3 by flowing 10% NH_3/N_2 at 100 °C for 30 min and then flushed with pure helium (30 mL min^{-1}) for 1 h. NH_3-TPD analysis was carried out with a ramp of 10 °C min^{-1} from 100 to 1000 °C under He flow of 30 mL min^{-1}.

TEM images of the fresh and used catalysts were obtained by using FEI (Technai F20 G2, The Netherlands) microscopy under STEM mode.

A TGA SDT-Q600 TA Instrument was used to investigate the carbon deposition of spent catalysts. The sample was heated from room temperature to 1000 °C at the rate of 10 °C min^{-1} in air (100 mL min^{-1}).

2.3. Steam Reforming of Glycerol. Steam reforming of glycerol was carried out in a fixed-bed down flow reactor at atmospheric pressure. In a typical experiment 500 mg of catalyst was prereduced in situ by flow of 10% H_2/N_2 for 2 h by placing at midpoint of the reactor. The mixture of steam-to-carbon (S/C) at a ratio of 3 was fed through an HPLC pump into a heated chamber (350 °C) to evaporate the solution completely before reaction. Gaseous products were analyzed by an online gas chromatograph (6890 N Agilent Technologies) with an automatic valve injection system. The glycerol conversion and hydrogen selectivity was calculated by the carbon balance method reported earlier.[40]

3. RESULTS AND DISCUSSION

X-ray diffraction patterns of perovskite type oxides and nickel supported alumina catalysts are presented in Figure 1. The

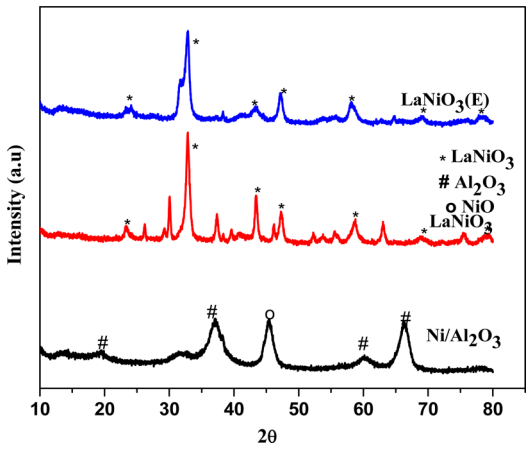

Figure 1. XRD patterns of fresh catalysts $LaNiO_3$ (E), $LaNiO_3$ and Ni/Al_2O_3.

Table 1. Physical Characterization of the Catalysts[a]

				NiO particle size in nm	
catalyst	S.A. (m^2/g)	P.V. (cm^3/g)	P.D. (nm)	before	after
$LaNiO_3$ (E)	10.7	0.09	3.4	9.3	10.6
$LaNiO_3$	15.0	0.07	4.1	12.6	12.9
Ni/Al_2O_3	110.0	0.32	11.8	12.5	12.3

[a]S.A., surface area; P.V., pore volume; P.D., pore diameter.

diffraction peaks at 2θ = 23.4, 32.7, 41.4, 47.1, 58.2, 68.1 and 78.3 are assigned to the $LaNiO_3$ rhombohedral phase (JCPDF: 10-0341), confirming the formation of perovskite type oxide catalyst.

The diffraction pattern of $LaNiO_3$ (E) is completely different from that of $LaNiO_3$. The main diffraction peaks for the rhombohedral $LaNiO_3$ appeared at 32.7, 47.1 and 58.2, (JCPDF 34-1028), which confirmed the presence of a perovskite-type structure. However, in $LaNiO_3$ the diffraction peaks slightly shifted toward a higher 2θ value with decreased peak intensity. In addition to this, other peaks are also detected. These additional peaks are assigned to characteristic peaks for the formation of La_2NiO_4 (JCPDF: 22-0712). La_2NiO_4 has a

DOI: 10.1021/acssuschemeng.6b01744
ACS Sustainable Chem. Eng. 2017, 5, 1339−1346

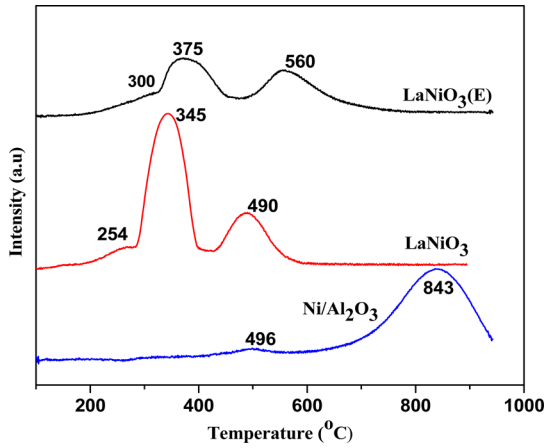

Figure 2. H_2-TPR profiles of $LaNiO_3$ (E), $LaNiO_3$ and Ni/Al_2O_3.

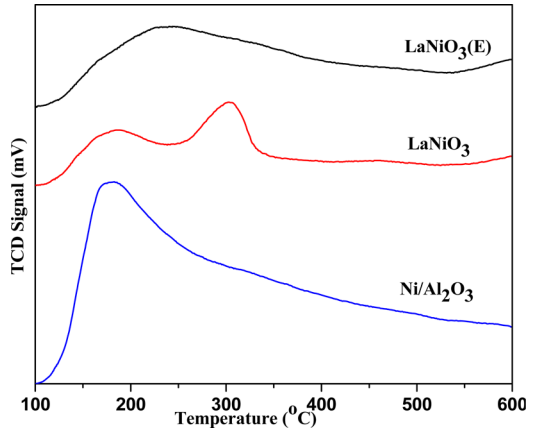

Figure 3. TPD-NH_3 profiles of $LaNiO_3$ (E), $LaNiO_3$ and Ni/Al_2O_3.

tetragonal structure and also belongs to the family of perovskite homologues with general formula A_2BO_4. This clearly indicates that only perovskite type $LaNiO_3$ formed when templates are used. So template can play an important role in the formation of perovskite structure.

The diffraction pattern for alumina supported nickel catalyst showed peaks at 2θ = 30.3, 46.8 and 66.7 which coincided with the nickel aluminate ($NiAl_2O_4$) spinel phase.[17] The peaks for NiO at 37.1, 46.5 and 66.7 are difficult to distinguish due to the overlap with the crystalline phase of Al_2O_3 and the $NiAl_2O_4$ peaks. However, the diffraction pattern shifted toward lower 2θ values with respect to reference values.[17] This may be due to the diffusion of NiO particles into the support structure and formation of the $NiAl_2O_4$ phase.

The inherent property of perovskite catalysts is the low specific surface area, and physical properties of perovskite and nickel supported alumina are reported in Table 1.

The prepared perovskite catalyst without using template showed higher surface area as compared to catalyst prepared with template. XRD results previously indicated that, along with the perovskite phase, additional phases were observed for $LaNiO_3$ catalysts which probably increase the total surface area. Nickel–alumina catalyst showed larger surface area with micropores. The average crystallite thickness of nickel oxide for all the catalysts were calculated using the Debye–Scherer equation and reported in Table 1. Perovskite catalyst with template resulted in slightly smaller nickel oxide particle size than the other.

Since Ni^0 crystallites are active species for steam reforming reaction, all the catalysts reduced with H_2 before reaction.[14,41] The reducibility of the prepared catalysts was investigated by H_2-TPR, and the reduction profiles are shown in Figure 2. The TPR profile of $LaNiO_3$ (E) showed two main reduction peaks at 375 and 560 °C, and the lower temperature peak with the shoulder at 300 °C is assigned to the reduction of $LaNiO_3$ to $La_4Ni_3O_{10}$, followed by La_2NiO_4.[39,42] The second peak corresponds to the reduction of La_2NiO_4 to Ni^0.[14,35] Similar reduction profiles were observed for the catalyst prepared without template ($LaNiO_3$); however, both the reduction peaks are shifted slightly toward lower temperature region. TPR results demonstrated that reduction of nickel in the perovskite structure is difficult at low temperature. The catalyst prepared without template showed intense reduction peaks and also increased hydrogen uptake, which is due to the development of different phases along with the perovskite phase.

Nickel supported alumina catalyst showed an intense reduction peak around 843 °C with the small peak at 496 °C, which is attributed to reduction of Ni^{2+} ions incorporated into tetrahedral and octahedral vacancies, respectively.[43−45] XRD analysis revealed that Ni supported alumina showed spinel phase formation in $NiAl_2O_4$, and it is very difficult to reduce nickel at lower temperature. Nickel particles are uniformly distributed over mesoporous alumina support, and there is a strong interaction between the nickel particle and the acidic alumina support, with the formation of nickel spinel at higher temperature resulting in higher reduction temperature (>843 °C).

The NH_3-TPD profiles of the catalysts in Figure 3 showed weak acidic sites for the perovskite derived catalysts, whereas Ni supported alumina possesses strong acid sites. $LaNiO_3$ showed two peaks, which are due to La_2NiO_4 species. The acid strength of the prepared catalysts decreased in the order of Ni/Al_2O_3 > $LaNiO_3$ > $LaNiO_3$ (E).

TEM images of the samples in Figure 4 showed that smaller nickel oxide particles are in close agreement with the average particle size as obtained by the XRD patterns (Table 1). Perovskite prepared using the template resulted in smaller particle size, whereas without template it resulted in slightly increased particle domains. Nickel supported alumina showed uniform distribution of nickel particles on the alumina support.

3.1. Catalytic Performance. The catalytic activity of the catalysts in the steam reforming of glycerol was measured, and the results are illustrated in Table 2. It was observed that $LaNiO_3$ (E) showed superior activity and selectivity compared to the other two catalysts, at both 550 and 650 °C temperatures. Earlier results suggested that perovskite catalyst $LaNiO_3$ (E) possesses highly active smaller nickel oxide particles which are responsible for the better catalytic performance. The perovskite prepared without template leads to slightly bigger particle which showed comparatively less glycerol conversion. TPR results clearly demonstrated that nickel in $LaNiO_3$ completely reduced during the activation period, and it was expected to show the good catalytic performance compared to $LaNiO_3$ (E).

Recently Wu et. al.[14] reported perovskite based catalyst for the hydrogen production by glycerol steam reforming, and they found almost 100% glycerol conversion with good H_2 selectivity; however, the catalyst showed quick deactivation due to carbon deposition.

In order to explore further, the effect of reaction temperature was studied at two different temperatures, since the steam

DOI: 10.1021/acssuschemeng.6b01744
ACS Sustainable Chem. Eng. 2017, 5, 1339−1346

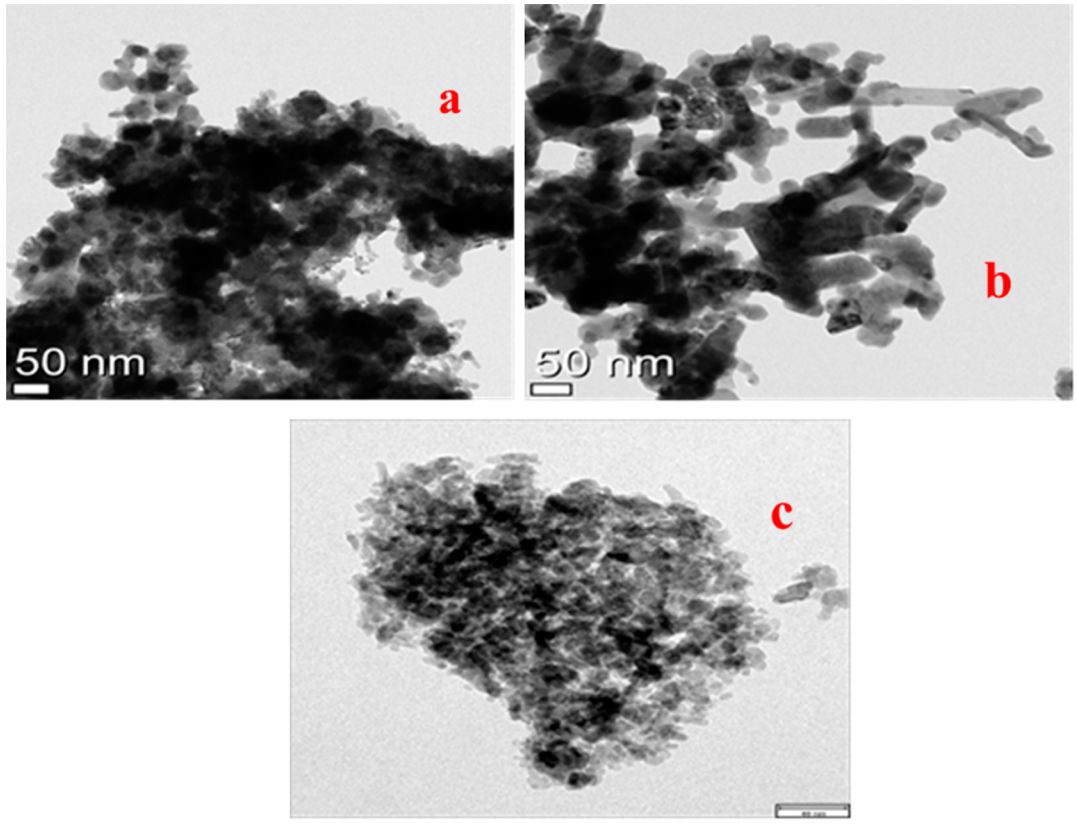

Figure 4. TEM images of fresh catalysts (a) $LaNiO_3$(E), (b) $LaNiO_3$ and (c) Ni/Al_2O_3.

Table 2. Catalytic Performance for Steam Reforming of Glycerol

		550 °C			650 °C		
		$LaNiO_3$ (E)	$LaNiO_3$	Ni/Al_2O_3	$LaNiO_3$ (E)	$LaNiO_3$	Ni/Al_2O_3
glycerol conversion (%)		48.4	41.2	5.4	72.04	68.3	56.4
selectivity (%)	H_2	70.3	68.5	66.8	69.6	65.9	67.8
	CO	1.3	0.3	12.3	4.1	2.7	4.4
	CH_4	0.8	1.3	1.4	2.4	3.5	2.8
	CO_2	28.1	29.9	19.5	23.9	27.9	25.0

reforming reaction is an endothermic reaction and activity is directly proportional to the temperature. With increase in reaction temperature from 550 to 650 °C, glycerol conversion increased for all three catalyst samples. But the $LaNiO_3$ (E) sample showed slightly higher conversion and selectivity than others (Table 2). The product distribution and selectivities also followed the same trend; however, with increase in temperature hydrogen selectivity should increase due to the endothermic nature of the reaction, but the reverse trend was observed which may be due to a lesser water gas shift reaction which was confirmed with increase in methane selectivity. Results revealed that acidity and nickel particle size of the catalysts play a crucial role in glycerol conversion and product selectivity.

Many researchers reported that Ni supported alumina acts as an active catalyst for the reforming reaction, but the drawbacks are quick deactivation, metal sintering and very high temperature requirement to reduce the nickel. It was observed that nickel supported alumina catalyst requires 843 °C to reduce Ni^{2+} to Ni^0, and this may be the reason for the very low activity. The metallic nickel is the active species for steam reforming, and hence all the catalysts were reduced with H_2 at 500 °C for 2 h before the reaction, because that temperature studied is not enough to reduce the nickel in the case of nickel supported alumina.

Under similar experimental conditions, the perovskite derived catalysts showed higher glycerol conversion. The acidic nature of the alumina support hinders the glycerol conversion and also leads to the formation of methane at both the temperatures studied. Under reactive conditions, perovskite prepared using template exhibiting smaller nickel oxide particle size with the least acidic sites showed better performance compared to the other two catalysts. For all catalysts, H_2 selectivity decreases slightly with increasing the reaction temperature from 550 to 650 °C, and this may be due to reduction in the water gas shift reaction at higher temperature; one has to decrease the acidic sites by incorporating another metallic promoter like Mg, Sr, and Ca^2 to the alumina support.

3.2. Catalytic Stability. In order to investigate the stability of prepared catalysts for steam reforming of glycerol, time on stream experiments were carried out at 650 °C with LHSV = 10000 h^{-1} and S/C = 3 for 24 h for all the three catalyst samples, and the results are represented in Figure 5. It showed that the catalysts are stable toward conversion and selectivity up to 24 h. In the case of nickel supported alumina catalyst,

DOI: 10.1021/acssuschemeng.6b01744
ACS Sustainable Chem. Eng. 2017, 5, 1339−1346

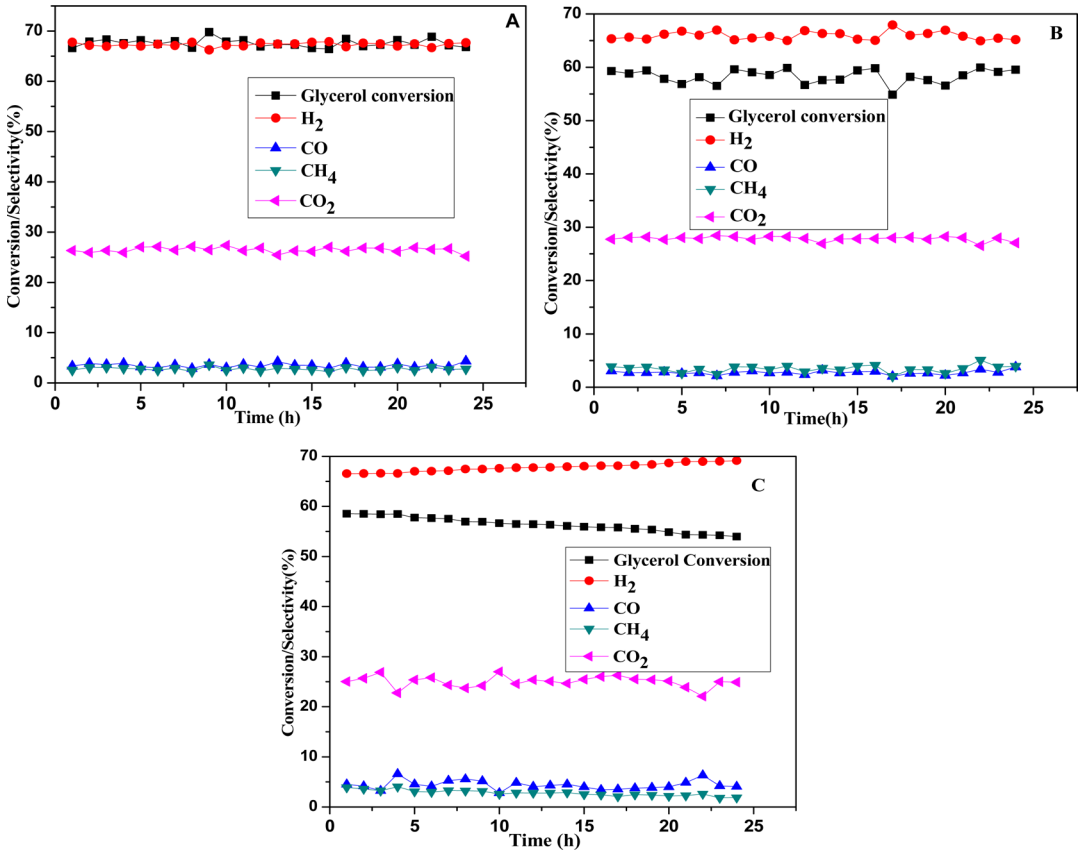

Figure 5. Stability of the catalysts (A) $LaNiO_3$ (E), (B) $LaNiO_3$ and (C) Ni/Al_2O_3.

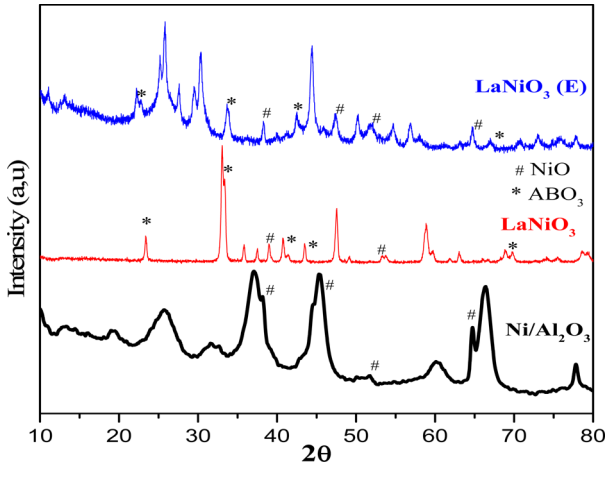

Figure 6. XRD diffraction patterns of spent catalysts $LaNiO_3$ (E), $LaNiO_3$ and Ni/Al_2O_3.

Table 3. TGA Results of Used Catalysts

catalyst	temperature (°C)	% wt loss
$LaNiO_3$ (E)	564–586	29.8
$LaNiO_3$	570–594	51.6
Ni/Al_2O_3	600	61.3

initially glycerol conversion was 59%, and it reduced gradually to 54% after 24 h; however, hydrogen selectivity increased from 67 to 69%. Whereas the selectivity of products and glycerol conversion over the $LaNiO_3$ (E) catalyst at 650 °C were stable up to 24 h on stream and deactivation phenomenon of the

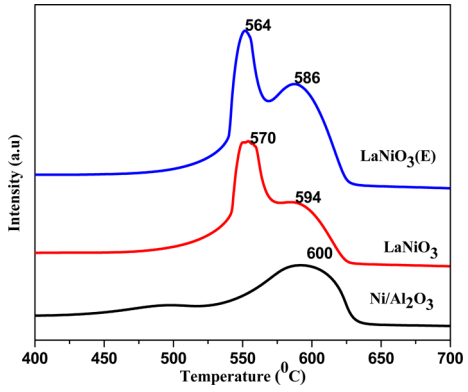

Figure 7. DTA profiles of used catalysts $LaNiO_3$ (E), $LaNiO_3$ and Ni/Al_2O_3.

catalyst was observed after 30 h, it is due to deposition of carbon on the catalyst through coke formation. While the $LaNiO_3$ sample showed catalytic stability the same as that of $LaNiO_3$ (E) without deactivation up to 30 h, the glycerol conversion and selectivity of products was slightly less compared to $LaNiO_3$ (E). In the case of Ni/Al_2O_3 there is continuous decreased glycerol conversion observed after 2 h from 59% to 53%, and after 25 to 30 h 14% of the conversion was decreased; this clearly indicated that the formation of coke is faster in the Ni/Al_2O_3 sample leading to quicker deactivation of catalysts than perovskite catalyst samples. This clearly demonstrates the superiority of perovskite catalysts compared to Ni supported alumina catalyst, because of smaller particle size of the nickel oxide, easy reduction of nickel, and moderately weak acidic sites. The coke formation on the

DOI: 10.1021/acssuschemeng.6b01744
ACS Sustainable Chem. Eng. 2017, 5, 1339–1346

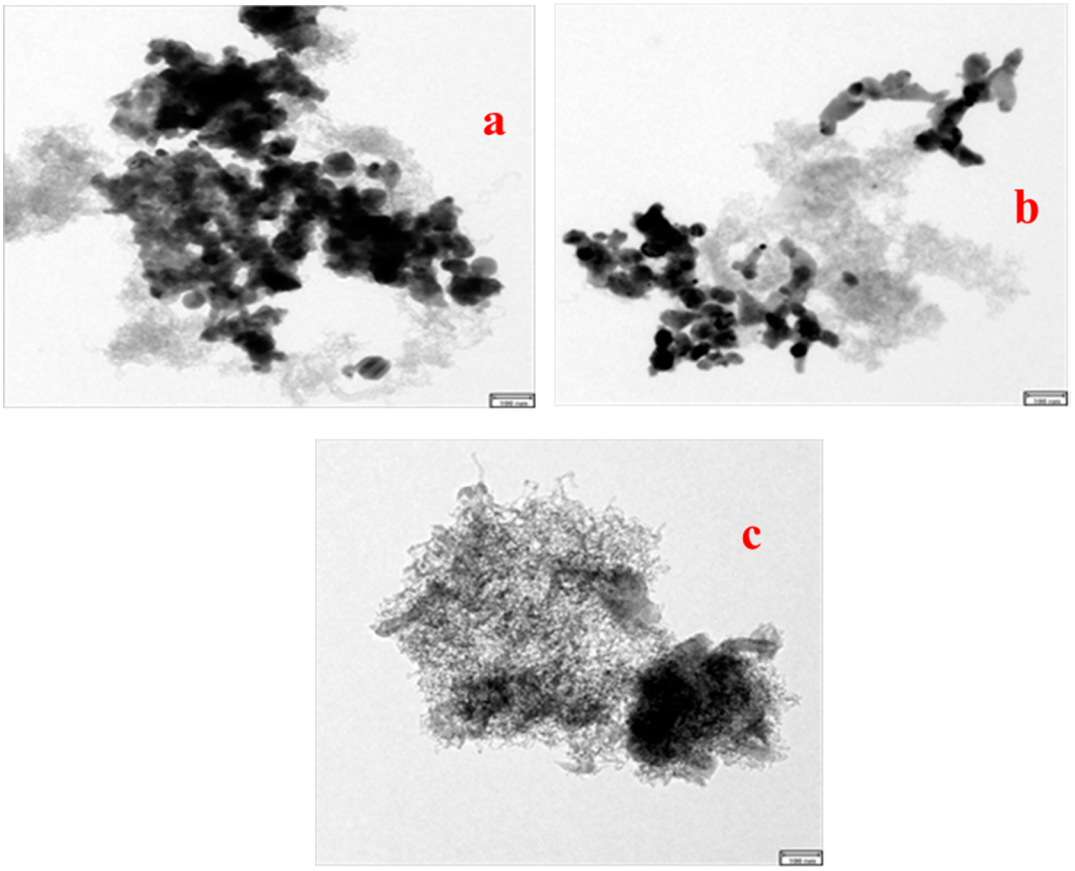

Figure 8. TEM images of used catalysts (a) $LaNiO_3$(E), (b) $LaNiO_3$ and (c) Ni/Al_2O_3.

catalyst samples was further confirmed by the analysis of spent catalysts and discussed in detail in the following section.

3.3. Characterization of the Spent Catalyst. After the stability test, the catalysts were collected and characterized to investigate the catalytic deactivation process during the course of reaction. Nickel-based catalysts are reported for their high reforming activity. However, short lifetime due to coke deposition, metal sintering and methane formation are drawbacks. To examine the deposition of coke during the reaction, the catalysts were collected and dried at 80 °C for 1 h and were subjected to analysis using XRD, TGA and TEM techniques. XRD patterns of spent perovskite derived Ni and Ni/Al_2O_3 catalysts are presented in Figure 6. The analysis of spent catalysts show that XRD patterns of all the samples were slightly different from the original (Figure 1). After the reaction perovskite catalysts show a changed $LaNiO_3$ to La_2O_3 phase with NiO. The XRD pattern showed main diffraction peaks at 29.9, 39.4, 46.0, 52.0 and 55.4 for the characteristic of La_2O_3 hexagonal structure (JCPDF 5-602). This La_2O_3 phase claimed to be responsible for the removal of carbonaceous material developed at the interface with the Ni crystallites. In addition to this carbon in the graphite and amorphous form, the carbon peaks at 25.6, 30.8, 44.6 and 78.2 (JCPDF 75-2078 and 72-2091) due to deposited coke leads to deactivation of catalyst. However, $LaNiO_3$ (E) showed pattern a completely different from the original and a slightly changed pattern from $LaNiO_3$, whereas the Ni/Al_2O_3 sample showed a slightly changed XRD pattern with carbon and NiO peaks in addition to $NiAl_2O_4$ spinel peaks.

The characteristic peaks of perovskite, Ni, and Al_2O_3 phases exist in the spent catalysts, and corresponding Ni particle size of all the catalysts are presented in (Table 1). However, two additional peaks were observed in the spent catalysts at 44.4 and 51.8 which are due to the formation of $La(OH)_3$ and Ni^0 phases as reported by Soongprasit et al.[46,47] At the beginning of the reaction, $LaNiO_3$ was converted to La_2O_3 and Ni^0 followed by recrystallization of reduced products (Ni^0 and La_2O_3). The lanthanum oxide obtained was further hydrolyzed to $La(OH)_3$. The reduction of Ni^{2+} to Ni^0 is expected due to hydrogenation during the glycerol steam reforming.

The amount of carbon deposited was quantitatively determined by TGA-DTA analysis, and the weight loss is shown in Table 3. The spent catalysts were first pretreated at 600 °C for 30 min before the TGA analysis in order to eliminate the influence of the potential carbonate. The mass of the catalysts initially increased due to the oxidation of Ni particles,[48,49] which confirmed the existence of Ni in used catalysts. From Table 3 it can be observed that the amount of coke deposition follows the order $LaNiO_3$ (29.8%) < $LaNiO_3$ (E) (33.6%) < Ni/Al_2O_3 (61.3%).

To eliminate the effect of nickel oxidation and to confirm the degree of coke deposition, TPO analysis was carried out, and the results are shown in Figure 7. It was observed that coke was deposited over all three catalysts. The deposited carbon undergoes oxidation in the temperature range of 470 to 620 °C. Calles et al.[50] reported that amorphous carbon oxidizes below 550 °C, whereas filamentous/graphitic carbon requires slightly high temperature for oxidation (600 °C). Perovskite derived catalysts showed two peaks with the intense peak at 490 °C due to amorphous carbon and less intense peak at 600 °C due to the small amount of graphitic carbon. During the stability tests, it was confirmed that perovskite catalysts are

DOI: 10.1021/acssuschemeng.6b01744
ACS Sustainable Chem. Eng. 2017, 5, 1339−1346

stable up to 24 h without losing activity.[51] However, nickel supported alumina catalyst showed only one broad peak at 600 °C indicating the large amount of graphitic carbon deposition. This was reflected in glycerol conversion which was dropped by 5% in 24 h. TGA results also confirmed the quick deactivation due to the deposition of filamentous carbon on surface active species. Perovskite derived catalysts hindered carbon deposition due to weak surface acidic sites with smaller nickel oxide particles, and the perovskite type oxide catalysts are capable of producing good dispersion of metallic particles upon reduction.[51] These small nickel particles give rise to strong metal−support interactions which could suppress carbon deposition and boost the catalyst activity.[12]

Further, all the used catalysts were examined by TEM, and the images are shown in Figure 8. Morphologies of the spent samples are almost similar to those of fresh perovskite catalysts (Figure 8A,B). However, carbon deposition is mostly in the amorphous form, and we did not observe the filamentous form, which was the one observed in the case of Ni/Al_2O_3 catalyst.

4. CONCLUSIONS

Perovskite type catalysts were prepared with and without using templates and showed better dispersion and reducibility of nickel with weakly acidic sites as compared to nickel supported alumina. $LaNiO_3$ (E) catalyst showed higher catalytic performance than both $LaNiO_3$ and Ni supported alumina catalyst, and the perovskite catalysts showed more catalytic stability than Ni/Al_2O_3 for reforming reactions, even though $LaNiO_3$ catalyst showed activity inferior to that of $LaNiO_3$(E) catalyst and excellent performance compared to Ni/Al_2O_3. Ni supported alumina showed quick deactivation of catalyst due to coke formation on the active sites. Perovskite derived catalysts with smaller nickel particle size and weak acidic sites are the best alternatives for the industrial hydrogen production by reforming reactions of glycerol.

AUTHOR INFORMATION

Corresponding Author

*(N.J.V.) E-mail: venkatesha.312@gmail.com. Ph: +91 99010 03120.

ORCID

N. J. Venkatesha: 0000-0002-9091-9744

Notes

The authors declare no competing financial interest.

ACKNOWLEDGMENTS

The authors thank the Rajya Vokkalighara sangha and Bangalore Institute of Technology for the analysis support.

REFERENCES

(1) Zou, J. J.; Zhang, Y. P.; Liu, C. J. Hydrogen production from partial oxidation of dimethyl ether using corona discharge plasma. *Int. J. Hydrogen Energy* **2007**, *32*, 958−964.

(2) Zhang, Y. H. P. Renewable carbohydrates are a potential high-density hydrogen carrier. *Int. J. Hydrogen Energy* **2010**, *35*, 10334−10342.

(3) Rahemi, N.; Haghighi, M.; Babaluo, A. A.; Jafari, M. F.; Allahyari, S. The effect of calcination tempaertaure on the Physico-Chemical properties and Catalytic activity in the dry reforming of methane over a Ni-Co/Al_2O_3−ZrO_2 nanocatalyst prepared by a Hybrid impregnation-plasma method. *Catal. Sci. Technol.* **2013**, *3*, 3183−3191.

(4) Chen, D.; He, L. Towards an Efficient Hydrogen Production from Biomass: A Review of Processes and Materials. *ChemCatChem* **2011**, *3*, 490−511.

(5) He, L.; Parra, J. M. S.; Blekkan, E. A.; Chen, D. Towards efficient hydrogen production from glycerol by sorption enhanced steam reforming. *Energy Environ. Sci.* **2010**, *3*, 1046−1056.

(6) Luo, W.; Asthagiri, A. An *ab initio* thermodynamics study of cobalt surface phases under ethanol steam reforming conditions. *Catal. Sci. Technol.* **2014**, *4*, 3379−3389.

(7) Chen, T.; Wu, C.; Liu, R. Steam reforming of bio-oil from rice husks fast pyrolysis for hydrogen production. *Bioresour. Technol.* **2011**, *102*, 9236−9240.

(8) Abello, S.; Bolshak, E.; Gispert-Guirado, F.; Farriol, X.; Montane, D. Ternary Ni−Al−Fe catalysts for ethanol steam reforming. *Catal. Sci. Technol.* **2014**, *4*, 1111−1122.

(9) Garcia, L.; French, R.; Czernik, S.; Chornet, E. Catalytic steam reforming of bio-oils for the production of hydrogen: effects of catalyst composition. *Appl. Catal., A* **2000**, *201*, 225−239.

(10) Bridgwater, A. V. Review of fast pyrolysis of *biomass* and product upgrading *Biomass* and Bioenergy. *Biomass Bioenergy* **2012**, *38*, 68−94.

(11) Soares, R. R.; Simonetti, D. A.; Dumesic, J. A. Glycerol as a Source for Fuels and Chemicals by Low-Temperature Catalytic Processing. *Angew. Chem., Int. Ed.* **2006**, *45*, 3982−3985.

(12) Kim, S. M.; Woo, S. I. Sustainable Production of Syngas from Biomass-Derived Glycerol by Steam Reforming over Highly Stable Ni/SiC. *ChemSusChem* **2012**, *5*, 1513−1522.

(13) Sanchez-Sanchez, M. C. S.; Navarro, R. M.; Fierro, J. L. G. Ethanol steam reforming over Ni/M_xO_y-Al_2O_3 (M = Ce, La, Zr and Mg) catalysts: Influence of support on the hydrogen production. *Int. J. Hydrogen Energy* **2007**, *32*, 1462−1471.

(14) Wu, G.; Li, S.; Zhang, C.; Wang, T.; Gong, J. Glycerol steam reforming over perovskite-derived nickel-based catalysts. *Appl. Catal., B* **2014**, *144*, 277−285.

(15) Chen, S. Q.; Liu, Y. $LaFeyNi_{1-}yO_3$ supported nickel catalysts used for steam reforming of ethanol. *Int. J. Hydrogen Energy* **2009**, *34*, 4735−4746.

(16) Boumaza, A.; Favaro, L.; Ledion, J.; Sattonnay, G.; Brubach, J. B.; Berthet, P.; Huntz, A. M.; Roy, P.; Tetot, R. Transition alumina phases induced by heat treatment of boehmite: An X-ray diffraction and infrared spectroscopy study. *J. Solid State Chem.* **2009**, *182*, 1171−1176.

(17) Maciver, D. S.; Tobim, H. H.; Barth, R. T. Catalytic aluminas I. Surface chemistry of eta and gamma alumina. *J. Catal.* **1963**, *2*, 485−497.

(18) (a) Chen, D.; Lodeng, R.; Anundskas, A.; Olsvik, O.; Holmen, A. Deactivation during carbon dioxide reforming of methane over Ni catalyst: microkinetic analysis. *Chem. Eng. Sci.* **2001**, *56*, 1371−1379. (b) Tian, H.; Li, X.; Zeng, L.; Gong, J. Recent Advances on the Design of Group VIII Base-metal Catalysts with Encapsulated Structures. *ACS Catal.* **2015**, *5*, 4959−4977.

(19) Bermudez, J. M.; Fidalgo, B.; Arenillas, A.; Menendez, J. A. CO_2 reforming of coke oven gas over a $Ni/\gamma Al_2O_3$ catalyst to produce syngas for methanol synthesis. *Fuel* **2012**, *94*, 197−203.

(20) (a) Bobadilla, L. F.; Alvarez, A.; Dominguez, M. I.; Romero-Sarria, F.; Centeno, M. A.; Montes, M.; Odriozola, J. A. Influence of the shape of Ni catalysts in the glycerol steam reforming. *Appl. Catal., B* **2012**, *123−124*, 379−390. (b) Li, S.; Gong, J. Strategies for improving the performance and stability of Ni-based catalysts for reforming reactions. *Chem. Soc. Rev.* **2014**, *43*, 7245−7256.

(21) Maluf, S. S.; Assaf, E. M. Ni catalysts with Mo promoter for methane steam reforming. *Fuel* **2009**, *88*, 1547−1553.

(22) Wu, P.; Li, X.; Ji, S.; Lang, B.; Habimana, F.; Li, C. Steam reforming of methane to hydrogen over Ni-based metal monolith catalysts. *Catal. Today* **2009**, *146*, 82−86.

(23) Choi, G. Y.; Kim, Y. C.; Moon, D. J.; Seo, G.; Park, N. C. Steam Reforming of Glycerol for Hydrogen Production Over Supported Nickel Catalysts on Alumina. *J. Nanosci. Nanotechnol.* **2013**, *13*, 653−656.

DOI: 10.1021/acssuschemeng.6b01744
ACS Sustainable Chem. Eng. 2017, 5, 1339−1346

(24) Moon, D. J. Hydrogen Production by Catalytic Reforming of Gaseous Hydrocarbons (Methane & LPG). *Catal. Surv. Asia* **2008**, *12*, 188−202.
(25) Seung-hoon, K.; Jae-sun, J.; Eun-hyeok, L.; Kwan-Young, L.; Dong Ju, M. Enhanced photocatalytic activity of TiO_2 thin films on plasma-pretreated organic polymers. *Catal. Today* **2014**, *228*, 145−151.
(26) Dou, B.; Wang, C.; Chen, H.; Song, Y.; Xie, B. Continuous sorption-enhanced steam reforming of glycerol to high-purity hydrogen production. *Int. J. Hydrogen Energy* **2013**, *38*, 11902−11909.
(27) Dieuzeide, M. L.; Jobbagy, M.; Amadeo, N. Glycerol steam reforming over Ni/γ-Al_2O_3 catalysts, modified with Mg(II). Effect of Mg (II) content. *Catal. Today* **2013**, *213*, 50−57.
(28) Cheng, C. K.; Foo, S. Y.; Adesina, A. A. Steam reforming of glycerol over Ni/Al_2O_3 catalyst. *Catal. Today* **2011**, *178*, 25−33.
(29) (a) Araque, M.; Martinez T, L. M.; Vargas, J. C.; Centeno, M. A.; Roger, A. C. Effect of the active metals on selective H_2 production in glycerol steam reforming. *Appl. Catal., B* **2012**, *125*, 556−566. (b) Wu, G.; Zhang, C.; Li, S.; Huang, Z.; Yan, S.; Wang, S.; Ma, X.; Gong, J. Sorption enhanced steam reforming of ethanol on Ni-CaO-Al_2O_3 multifunctional catalysts derived from hydrotalcite-like compounds. *Energy Environ. Sci.* **2012**, *5*, 8942−8949.
(30) Han, J. W.; Kim, C.; Park, J. S.; Lee, H. Highly Coke-resistant Ni nanoparticle catalysts with minimal sintering in dry reforming of methane. *ChemSusChem* **2014**, *7*, 451−456.
(31) de Lima, S. M.; da Silva, A. M.; da Costa, L. O. O.; Assaf, J. M.; Mattos, L. V.; Sarkari, R.; Venugopal, A.; Noronha, F. B. Hydrogen production through oxidative steam reforming of ethanol over Ni-based catalysts derived from $La_{1-x}Ce_xNiO_3$perovskite-type oxides. *Appl. Catal., B* **2012**, *121−122*, 1−9.
(32) Barbero, B. P.; Gamboa, J. A.; Cadus, L. E. Synthesis and characterization of $La_{1-x}CaxFeO_3$ perovskite-type oxide catalysts for total oxidation of volatile organic compounds. *Appl. Catal., B* **2006**, *65*, 21−30.
(33) Glisenti, A.; Galenda, A.; Natile, M. M. Steam reforming and oxidative steam reforming of methanol and ethanol: The behaviour of $LaCo_{0.7}Cu_{0.3}O_3$. *Appl. Catal., A* **2013**, *453*, 102−112.
(34) Navarro, R. M.; Alvarez-Galvan, M. C.; Villoria, J. A.; González-Jiménez, I. D.; Rosa, F.; Fierro, J. L. G. Effect of Ru on $LaCoO_3$ perovskite-derived catalyst properties tested in oxidative reforming of diesel. *Appl. Catal., B* **2007**, *73*, 247−258.
(35) Valderrama, G.; Goldwasser, M. R.; Urbina de Navarro, C.; Tatibouet, J. M.; Barrault, J.; Batiot-Dupeyrat, C.; Martinez, F. Dry reforming of methane over Ni perovskite type oxides. *Catal. Today* **2005**, *107*, 785−791.
(36) Gallego, G. S.; Mondragon, F.; Barrault, J.; Tatibouet, J. M.; Batiot-Dupeyrat, C. B. CO_2 reforming of CH_4 over La−Ni based perovskite precursors. *Appl. Catal., A* **2006**, *311*, 164−171.
(37) Pereniguez, R.; González-DelaCruz, V. M.; Holgado, J. P.; Caballero, A. Synthesis and characterization of a LaNiO3 perovskite as precursor for methane reforming reactions catalysts. *Appl. Catal., B* **2010**, *93*, 346−353.
(38) Gallego, G. S.; Batiot-Dupeyrat, C. B.; Barrault, J.; Florez, E.; Mondragon, F. Dry reforming of methane over $LaNi_{1-y}B_yO_{3\pm\delta}$ (B = Mg, Co) perovskites used as catalyst precursor. *Appl. Catal., A* **2008**, *334*, 251−258.
(39) Cui, Y.; Galvita, V.; Rihko-Struckmann, L.; Lorenz, H.; Sundmacher, K. Steam reforming of glycerol: The experimental activity of $La_{1-x}CexNiO_3$ catalyst in comparison to the thermodynamic reaction equilibrium. *Appl. Catal., B* **2009**, *90*, 29−37.
(40) Dieuzeide, M. L.; Iannibelli, V.; Jobbagy, M.; Amadeo, N. Steam reforming of glycerol over Ni/Mg/γ-Al_2O_3 catalysts. Effect of calcination temperatures. *Int. J. Hydrogen Energy* **2012**, *37*, 14926−14930.
(41) de Lima, S. M.; Pena, M. A.; Fierro, J. L. G.; Assaf, J. M. La_{1-x} Ca $_x$ NiO_3 Perovskite Oxides: Characterization and Catalytic Reactivity in Dry Reforming of Methane. *Catal. Lett.* **2008**, *124*, 195−203.
(42) Liu, J. Y.; Su, W. N.; Rick, J.; Yang, S. C.; Cheng, J. H.; Pan, C. J.; Lee, J. F.; Hwang, B. J. Hierarchical Copper-Decorated Nickel Nanocatalysts Supported on La_2O_3 for Low-Temperature Steam Reforming of Ethanol. *ChemSusChem* **2014**, *7*, 570−576.
(43) Wu, M.; Hercules, D. M. Studies of supported nickel catalysts by x-ray photoelectron and ion scattering spectroscopies. *J. Phys. Chem.* **1979**, *83*, 2003−2008.
(44) Zhang, L.; Lin, J.; Chen, Y. Characterization of dispersion and surface states of NiO/γ-alumina and NiO/La_2O_3−γ-alumina catalysts. *J. Chem. Soc., Faraday Trans.* **1992**, *88*, 497−502.
(45) Wu, G.; Zhang, C.; Li, S.; Han, Z.; Wang, T.; Ma, X.; Gong, J. Hydrogen Production via Glycerol Steam Reforming over Ni/Al_2O_3: Influence of Nickel Precursors. *ACS Sustainable Chem. Eng.* **2013**, *1*, 1052−1062.
(46) Choudhary, V. R.; Uphade, B. S.; Belhekar, A. A. Oxidative Conversion of Methane to Syngas over $LaNiO_3$ Perovskite with or without Simultaneous Steam and CO_2 Reforming Reactions: Influence of Partial Substitution of La and Ni. *J. Catal.* **1996**, *163*, 312−318.
(47) Soongprasit, K.; Aht-Ong, D.; Sricharoenchaikul, V.; Atong, D. Synthesis and catalytic activity of sol-gel derived La−Ce−Ni perovskite mixed oxide on steam reforming of toluene. *Current Appl. Phys.* **2012**, *12*, S80−S88.
(48) Qi, X.; Guo, X.; Zheng, C. Density functional study the interaction of oxygen molecule with defect sites of graphene. *Appl. Surf. Sci.* **2012**, *259*, 195−200.
(49) Park, C.; Keane, M. A. Catalyst support effects in the growth of structured carbon from the decomposition of ethylene over nickel. *J. Catal.* **2004**, *221*, 386−399.
(50) Calles, J. A.; Carrero, A.; Vizcaíno, A. J.; García-Moreno, L. Hydrogen production by glycerol steam reforming over SBA-15-supported nickel catalysts: Effect of alkaline earth promoters on activity and stability. *Catal. Today* **2014**, *227*, 198−206.
(51) Franchini, C. A.; Aranzaez, W.; Duarte de Farias, A. M.; Pecchi, G.; Fraga, M. A. Ce-substituted $LaNiO_3$ mixed oxides as catalyst precursors for glycerol steam reforming. *Appl. Catal., B* **2014**, *147*, 193−202.

DOI: 10.1021/acssuschemeng.6b01744
ACS Sustainable Chem. Eng. 2017, 5, 1339−1346